Cellular Signalling 22 (2010) 1124–1131

Contents lists available at ScienceDirect

Cellular Signalling

journal homepage: www.elsevier.com/locate/cellsig

Pleiotropic role of Rac in mast cell activation revealed by a cell permeable *Bordetella* dermonecrotic fusion toxin

Heidi Stratmann, Carsten Schwan, Joachim H.C. Orth, Gudula Schmidt, Klaus Aktories *

Institut für Experimentelle und Klinische Pharmakologie und Toxikologie, Albert-Ludwigs-Universität Freiburg, Germany

ARTICLE INFO

Article history:
Received 17 February 2010
Accepted 1 March 2010
Available online 6 March 2010

Keywords:
Mast cell
Rac
Dermonecrotic toxin
TAT fusion protein
Phospholipase Cγ
Calcium

ABSTRACT

To activate the GTPase Rac in rat basophilic leukemia (RBL) cells and mouse bone marrow-derived mast cells (BMMC) a TAT fusion toxin of *Bordetella* dermonecrotic toxin (DNT-TAT) was constructed. The fusion toxin activated Rac1 and RhoA *in vitro* but only Rac in RBL cells and BMMC. DNT-TAT caused an increase in inositol phosphate formation, calcium mobilization, ERK activation and degranulation of mast cells. All these effects were inhibited by the Rho GTPase-inactivating *Clostridium difficile* toxin B and *Clostridium sordellii* lethal toxin. Also the calcium ionophore A23187 caused mast cell activation, including ERK phosphorylation, by processes involving an activation of Rac. The data indicate pleiotropic functions of Rac in mast cell activation.

1. Introduction

Antigen-induced cross-linking of the high affinity IgE receptor (FcεRI) induces an activation of mast cells with release of preformed mediators such as histamine, tryptase, proteoglycans and synthesis of prostaglandins, leukotriens and cytokines [1,2]. One basic event in FcεRI signaling is the activation of the Lyn pathway, resulting in Syk activation and phosphorylation of the adaptor proteins LAT and SLP76, activation of phospholipase Cγ (PLCγ) and mobilization of calcium [3]. Another complementary pathway induced by cross-linking of FcεRI starts with an activation of Fyn, depends on the adaptor protein GRB2 and involves PI3-kinase-dependent activation of protein kinase Cδ [4]. This pathway, which also appears to be essential for degranulation and Ca^{2+} amplification, may also receive an input from the Lyn pathway.

The signal protein complexes formed by LAT and SLP76 include Vav1, which activates the GTP-binding protein Rac [5]. Rac has been shown to be essential for PLCγ activation in mast cells [6,7]. The GTPase Rac belongs to the family of Rho proteins, which include ~20 mammalian proteins that act as molecular switches [8,9]. The GTPase Rac is inactive in the GDP-bound form and is activated by guanine nucleotide exchange factors (GEFs) like Vav, which induce the release of GDP and allow the binding of GTP. In the GTP-bound form, Rac activates various types of effectors, including PLCγ in mast cells. The active state of Rac is terminated by GTP hydrolysis, a process which is facilitated by GTPase-activating proteins (GAPs) [10,11].

Rho proteins, including RhoA, Rac1, and Cdc42, are the target of various bacterial protein toxins, which inactivate or activate the GTPases [12–14]. For example, Rac1, RhoA and Cdc42 are inhibited by *Clostridium difficile* toxin B [15]. *Clostridium sordellii* lethal toxin also inhibits Rac but not RhoA or Cdc42 [16]. Both toxins glucosylate the GTPases at threonine-35 (Rac or Cdc42) or threonine-38 (RhoA) and, thereby, prevent the conformational change into the active state of the GTPases. By contrast, Rac1 (and other Rho proteins) are activated by *E. coli* cytotoxic necrotizing factor (CNF) [17,18] and *Bordetella* dermonecrotic toxin (DNT) [19], which deamidate and/or transglutaminate the Rho proteins at a specific glutamine residue (e.g., glutamine-61 of Rac1 and glutamine-63 of RhoA). This modification constitutively activates the GTPases by preventing the hydrolysis of GTP.

To study Rac-dependent signaling pathways independently of cross-linking of FcεRI, we investigated the effects of Rac-activating toxins in rat basophilic leukemia (RBL) cells and mouse bone marrow-derived mast cells (BMMC). Because CNFs and DNT are not taken up by most hematopoetic cells, including mast cells, we employed a TAT construct, which is capable of entering mast cells. Here we report that

Abbreviation: BMMC, bone marrow-derived mast cells; CRAC channel, calcium release-activated calcium channels; DNT-TAT, TAT fusion toxin of *Bordetella* dermonecrotic toxin; DNT^{mut}-TAT, inactive mutant of DNT-TAT; ERK, extracellular signal-regulated kinase; FcεRI, high affinity IgE receptor; $InsP_3$, inositol trisphosphate; PLCγ, phospholipase Cγ.

* Corresponding author. Institut für Experimentelle und Klinische Pharmakologie und Toxikologie, Albertstraße 25, D-79104 Freiburg, Germany. Tel.: +49 761 2035301; fax: +49 761 2035311.
E-mail address: Klaus.Aktories@pharmakol.uni-freiburg.de (K. Aktories).

0898-6568/$ – see front matter © 2010 Elsevier Inc. All rights reserved.
doi:10.1016/j.cellsig.2010.03.007

Rac activation in RBL and mast cells by DNT-TAT causes PLC activation, calcium mobilization and degranulation.

2. Experimental procedures

2.1. Materials

C. difficile toxin B and *C. sordellii* lethal toxin were prepared as described [20]. A23187 was obtained from Sigma (Deisenhofen, Germany). The pTAT-HA plasmid was a gift from Dr. M. Lerm (Linköping, Sweden). The cell permeable inositol trisphosphate ($InsP_3$) analog $Bt_3Ins(1,3,4)P_3$ AM was from Alexis Biochemicals (Lörrach, Germany). TNP conjugates of hen egg ovalbumin were made using 2,4,6-trinitrobenzene sulfonic acid according to the method of Eisen et al. [21]. Recombinant RhoA and Rac1 were prepared from their fusion proteins (for example, RhoA-GST) as described [22]. All other reagents were of analytical grade and commercially available.

2.2. Cell culture

Rat basophilic leukemia (RBL) cells were grown in Eagle's MEM containing 10% fetal calf serum, 4 mM glutamine, 100 U/ml penicillin and streptomycin. RBL cells were detached from culture plates with SK buffer (125 mM NaCl, 1.5 mM EDTA, 5.6 mM glucose, and 10 mM HEPES, pH 7.2).

2.3. Preparation of bone marrow-derived mast cells (BMMC)

Mice were dispatched by CO_2. The bone marrow from femoral bone was washed out and cultivated in RPMI medium, containing 20% fetal calf serum, 1% X63Ag8-653-conditioned medium as source of IL-3 [23], 50 U/ml penicillin and streptomycin and 0.1 mM non-essential amino acids.

2.4. Construction of DNT-TAT and mutagenesis

The C-terminal domain (amino acid 1136–1451) of DNT (ΔDNT) was amplified by PCR from ΔDNT in pGEX-vector and restriction sites for XhoI and EcoRI were introduced. Sense primer DNT: 5′-GGA TCC GCT TCC GGC GGG GGG CCG-3′; antisense primer DNT: 5′-GGT ACC TCA GAC CGG CGC CGG AAA CAA C-3′.The PCR product was cloned into cloning vector pcr-Blunt II TOPO and introduced in TOP10 F′ *E. coli* (Invitrogen). After analysis for the correct gene sequence (Dye Terminator Cycle sequencing kit, Applied Biosystems) DNA was digested with XhoI and EcoRI (New England Biolabs) and the DNT-fragment ligated into pTAT-HA vector. The ligation product, DNT-TAT, was introduced in TG1 *E. coli*.

To get an inactive mutant of the DNT-TAT construct, a site-directed mutagenesis using a QuikChange kit (Stratagene) was performed. In DNT-TAT, cysteine-1296 of ΔDNT was changed to serine. Sense primer: DNT^{mut}: 5′-GGC TCC TTG AGC GGG TCC ACG ACG ATG GTT GGG-3′; antisense primer: DNT^{mut}: 5′-CCC AAC CAT CGT GGA CCC GCT CAA GGA GCC-3′.The mutated, DNT^{mut}-TAT, construct was checked by DNA sequencing.

2.5. Preparation of TAT proteins

TAT proteins, which contain an additional His_6-tag, were expressed in *E. coli* BL21 cells for 7 h at 37 °C. After centrifugation (10 min, 6000× g) cells were lysed in buffer Z (8 M urea, 100 mM NaCl and 20 mM Hepes, pH 8) with 10 mM imidazol and sonicated on ice. The lysate was centrifuged for 20 min at 15,000× g at 4 °C and supernatant incubated with Talon beads (Clontech Laboratories Inc.) for 2 h at 4 °C. After incubation, beads were washed with buffer Z and the TAT proteins were eluted with imidazol (100 mM–1 M). To remove urea and imidazol, a dialysis in Tris-buffered solution was performed over night at 4 °C. DNT-TAT and the inactive DNT^{mut}-TAT were stored up to 4 days at 4 °C on ice.

2.6. Hexosaminidase release assay

Hexosaminidase release was determined as described [24]. Where needed, cells were labelled with IgE (1% mouse anti-TNP-ovalbumin IgE-conditioned medium, overnight) and pretreated with toxins or inhibitors for the indicated times and concentrations. Thereafter, the medium was removed and cells were washed with PBS and resuspended in 100 µl tyrode buffer (130 mM NaCl, 5 mM KCl, 1.4 mM $CaCl_2$, 1 mM $MgCl_2$, 5.6 mM glucose, 10 mM HEPES and 0.1% BSA, pH 7.4). Then, cells were incubated with various stimuli for the indicated times and concentrations at 37 °C. Thereafter, 50 µl of the supernatant was incubated with 50 µl of 1.3 mg/ml p-nitrophenyl-N-acetyl-β-D-glucosaminide in 0.1 M sodium citrate buffer (pH 4.5) at 37 °C for 1 h. To stop the reaction, 100 µl of 0.4 M glycine (pH 10.7) was added. The total amount of hexosaminidase release was determined using 2% Triton X-100 in tyrode buffer. Absorbance was measured at 410 nm, referring to 630 nm. Results are shown in relation to untreated cells and calculated to antigen-induced or maximal DNT-TAT-induced hexosaminidase release.

2.7. Calcium imaging

RBL cells were seeded in glass-bottom culture dishes, pretreated as described and loaded with Fura-2 acetoxymethylester (Fura-2AM; 2.5 µM) for 0.5 h at 37 °C. After loading, cells were washed and the medium was replaced. 4 min after the start of calcium imaging cells were stimulated. For calcium imaging, pictures were acquired with a 40× objective (NA: 1.4) every 5 s. Fura-2AM was excited at 340 nm and 380 nm. Emission was detected at 510 nm. After rationing of both channels by Metamorph software (Universal Imaging, Downingtown, PA) different treatment groups were compared in their calcium-signals. Results are presented as an increase in changes in fluorescence ratio 340/380 nm over time.

2.8. Effector pull-down experiments

GST-PAK-Crib domain (amino acids 56–272) and GST-N-terminal rhotekin-domain (N-terminal 90 amino acids) were expressed as described before [25]. To detect the activation of RhoA or Rac, cells or cellular fractions were incubated and activated as described at 37 °C. After addition of 100 µl of ice-cold GST lysis buffer (10% glycerol, 50 mM Tris, pH 7.4, 100 mM NaCl, 1% (v/v) Nonidet P-40, 2 mM $MgCl_2$ and 0.1 mM phenylmethylsulfonyl fluoride), cells were scraped off and centrifuged at 14,000 rpm for 20 min at 4 °C. Afterwards, detergent-soluble supernatant was recovered; GTP-Rac/GTP-Rho proteins were precipitated at 4 °C for 1 h. The complexes were washed 3 times with ice-cold lysis buffer, resuspended and boiled with Laemmli buffer. Bound Rac/Rho proteins were detected by Western blotting using specific antibodies against Rac (Invitrogen) or RhoA (Santa Cruz), respectively. Binding of the second horseradish peroxidase-coupled antibody was detected with an enhanced chemi-luminescent detection reagent (100 mM Tris–HCl, pH 8.0, 1 mM luminol (Fluka), 0.2 mM p-coumaric acid, and 3 mM H_2O_2), and the imaging system LAS-3000 (Fujifilm). Quantification was performed by measuring band intensity normalized to control (Multi Gauge V3.0), determined from three independent experiments.

2.9. Detection of Rac- and Rho-transglutamination and deamidation in vitro

Recombinant RhoA and Rac1 were incubated with DNT-TAT or CNF1 for 3 h. The reaction mix contained 10% (v/v) TG buffer (80 mM $CaCl_2$, 1 mM EDTA, 50 mM $MgCl_2$, and 50 mM Tris pH 7.4), 1 mM

dithiothreitol, 12% (v/v) of an oversaturated solution of fluorescent dansylcadaverine (Sigma-Aldrich) in 50 mM Tris (pH 9), 5 µg Rac1 or RhoA and 2.5 µg DNT-TAT or CNF1. The probe volume was 20 µl. The reaction mix was incubated at 30 °C (DNT-TAT) or 37 °C (CNF1), respectively for the indicated time. To stop the reaction, Laemmli buffer was added and a SDS-PAGE performed. The fluorescently labelled proteins were visualized under UV light. Thereafter, the SDS gel was stained with Coomassie brilliant blue R-250.

2.10. Rhodamine-phalloidin-staining of RBL cells (F-actin staining)

After treatment with toxins, cells were washed, fixed and permeabilized (9.7% parafomaldehyde, and 0.1% Triton X-100 in PBS) for 10 min at room temperature. Cells were incubated with rhodamine phalloidin solution (Sigma) for 1 h at room temperature and after washing with PBS, cover slips were fixed on an object slide with ProLong gold antifade reagent containing DAPI (Invitrogen). Fluorescence was analyzed with an Axiophot microscope (Zeiss, 100× objective).

2.11. Measurement of inositol phosphates

BMMC were incubated with 4 µCi/ml [2-^{3}H] inositol in MEM medium overnight. Where needed, cells were incubated with 1% anti-TNP-ovalbumin IgE-conditioned medium. Cells were treated as described. To allow an accumulation of inositol phosphates, lithium chloride (20 mM) was added before the stimulation. The reaction was stopped by centrifugation and replacement of medium by cold formic acid (10 mM) and incubated for 1 h at 4 °C. After neutralizing with NH_3 (5 mM, pH 8–9) the inositols and total inositol phosphates were analyzed by anion exchange chromatography as described before [26]. Statistical significance was assessed using a paired *t*-test, with $^*p<0.05$.

2.12. Determination of ERK phosphorylation

BMMC were pretreated with toxins as indicated and, thereafter, stimulated for the indicated times and concentrations at 37 °C. The cells were washed once with ice-cold phosphate-buffered saline, lysed with RIPA-buffer (10 mM NaF, 5 mM EDTA, 10 mM Na-phosphate-buffer, 5% ethylene glycol, 50 mM HEPES, 150 mM NaCl, 1% Triton X-100, 0.5% Na-deoxycholate, 0.1% SDS, and complete protease inhibitor (Roche), pH 7.4) and sonicated on ice. Cell lysates were separated by SDS-PAGE, and phosphorylation was determined by subsequent immunoblotting with a phosphospecific anti-ERK antibody (Santa Cruz Biotechnology). Aliquots of total lysates were used to check equal loading by anti-ERK antibody (Santa Cruz Biotechnology). Quantification was performed by measuring band intensity normalized to control (Multi Gauge V3.0), determined from three independent experiments.

2.13. Live cell imaging

For live cell imaging, cells were stimulated as indicated and observed in a chamber that provided a humidified atmosphere (6.5% CO_2, and 9% O_2) at 37 °C on a Zeiss Axiovert 200 M inverted microscope. Images were collected with a digital camera (Coolsnap HQ, Roper Scientific) driven by Metamorph imaging software (Universal Imaging). For DIC-Imaging pictures were acquired with a 40× objective (NA: 1.4) every 30 s.

3. Results

Bacterial protein toxins are widely used as high specific tools in cell biology or biochemistry. Here we utilized the GTPase-activating bacterial protein toxins CNF1 and DNT to investigate the role of small GTPases in mast cell activation. Initial studies showed that CNF1 is not taken up by mast cells. Also a CNF1-TAT fusion protein did not activate Rho proteins in mast cells either (not shown). Therefore, we constructed a fusion protein, consisting of the catalytic domain of DNT and TAT peptide (here called DNT-TAT). To distinguish the biological effects of the catalytic domain of DNT from the effects induced by the TAT peptide, we also constructed an inactive DNT-TAT fusion protein (DNT^{mut}-TAT), in which the catalytic cysteine residue (cysteine-1296) of DNT was changed to serine. Both proteins were very well expressed and highly purified (data not shown).

3.1. Activation of Rho GTPases by DNT-TAT

At first, we studied the effects of DNT-TAT on recombinant RhoA and Rac1 and compared it with CNF1 *in vitro*. As found for the deamidating CNF1, treatment of RhoA with DNT-TAT caused a shift in the apparent molecular mass of the GTPase on SDS-PAGE. This shift is due to deamidation of RhoA at glutamine-63 (Fig. 1A). Deamidation was not observed with the inactive DNT^{mut}-TAT. In addition to the deamidating activity, DNT but not CNF1 possesses transglutamination activity. This activity of DNT-TAT was studied in the presence of dansylcadaverine [27]. As shown in Fig. 1A, DNT-TAT caused the dansylation of RhoA and Rac1, whereas the inactive mutant DNT^{mut}-TAT or CNF1 did not transglutaminate Rho proteins under these conditions.

Treatment of intact RBL cells with DNT-TAT caused strong effects on the cytoskeleton and the morphology of RBL cells. Rhodamine-phalloidin-staining revealed DNT-TAT-induced strong membrane ruffling, formation of lamellipodia, spreading and flattening of cells (Fig. 2A). Besides lamellipodia formation, life imaging showed a

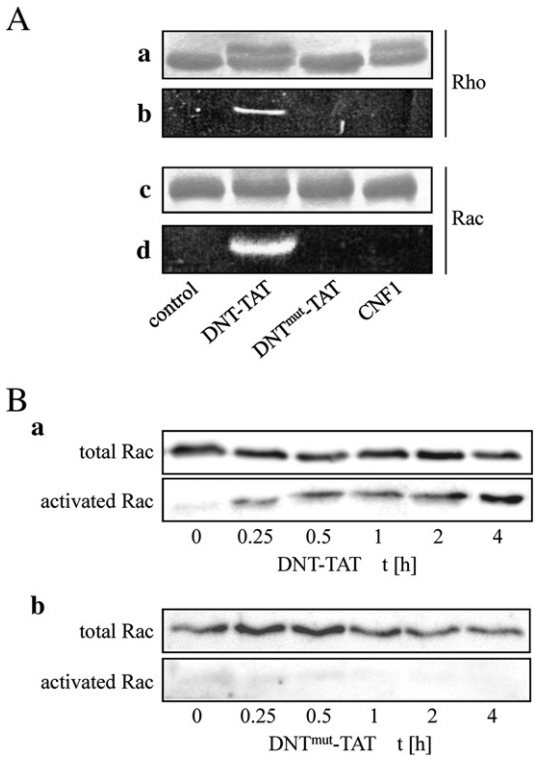

Fig. 1. Activation of Rho GTPases by DNT-TAT. A. Recombinant Rac1 and RhoA proteins were incubated with DNT-TAT, the inactive mutant DNT^{mut}-TAT or CNF1 (each 2.5 µg), respectively, and fluorescent dansylcadaverine for 3 h. A SDS-urea-PAGE was performed and fluorescence detected by eagle eye imaging system (Stratagene) (b, d) and Coomassie-staining was performed (a, c), subsequently. B. BMMC were incubated with 300 nM DNT-TAT (a) or the inactive mutant (b) for indicated times and an effector pull-down assay and a Western blot were performed to monitor Rac activation. A fraction of total protein mixture was used to demonstrate equal loading. Rac was detected by a specific antibody.

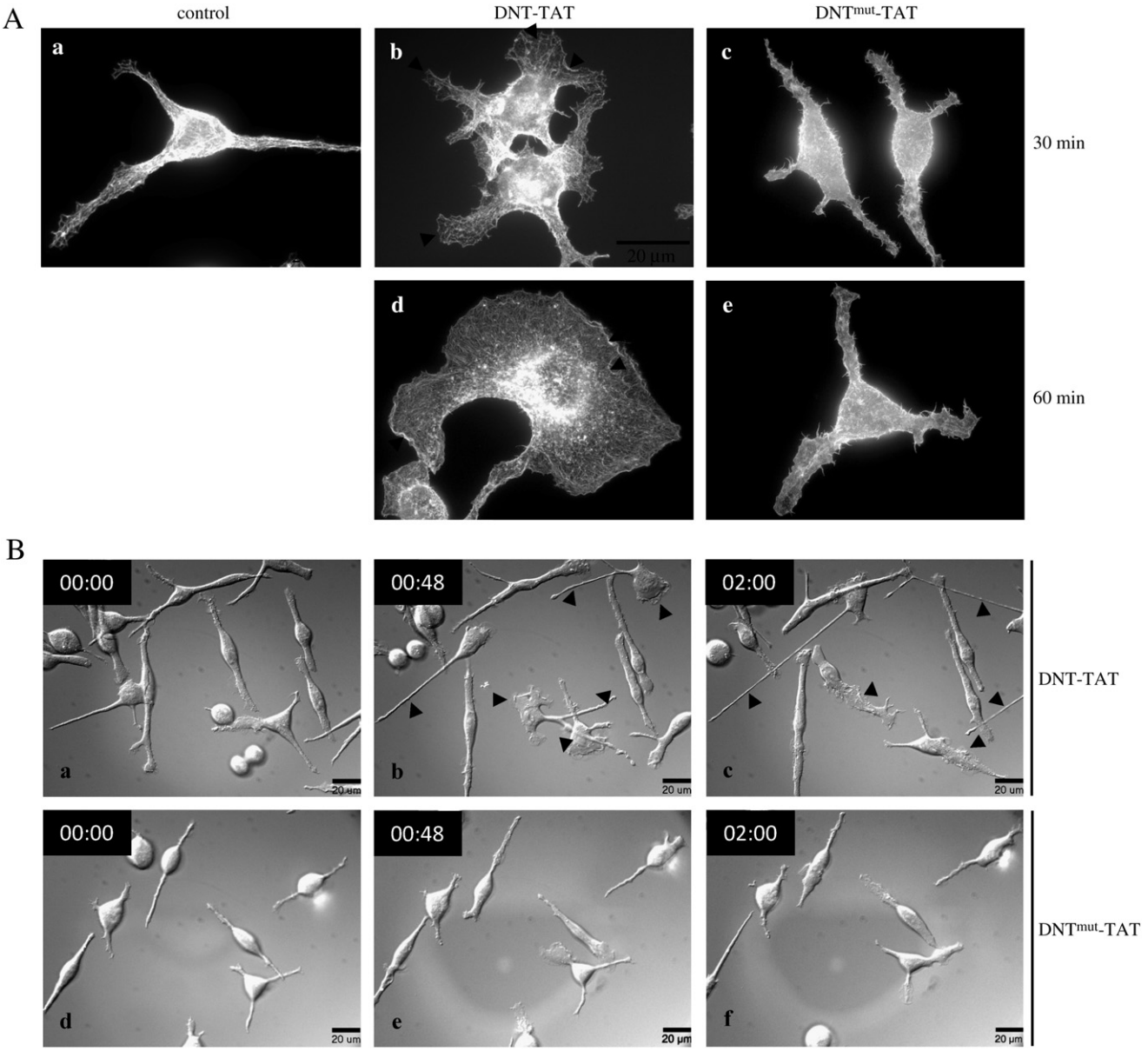

Fig. 2. Influence of DNT-TAT on actin cytoskeleton and cell morphology. A. RBL cells were stimulated for 30 and 60 min with DNT-TAT or the inactive mutant DNT^{mut}-TAT (300 nM), respectively. Rhodamine-phalloidin-staining was performed and fluorescence was analyzed by microscopy. Note the formation of lamellipodia and membrane ruffles after treatment with DNT-TAT (arrows). a) RBL cells untreated; b) 300 nM DNT-TAT, 30 min; c) 300 nM DNT^{mut}-TAT; d) 300 nM DNT-TAT, 60 min, 30 min; e) 300 nM DNT^{mut}-TAT, 60 min. B. 4 min after the start of live cell imaging, RBL cells were stimulated with 200 nM DNT-TAT or the inactive mutant, respectively. Images were collected with a digital camera driven by Metamorph imaging software. For DIC-Imaging pictures were acquired with a 40× objective (NA: 1.4) every 30 s. Cells were photographed before stimulation (a, d) and 48 min (b, e) and 2 h (c, f) after stimulation.

formation of long extensions (Fig. 2B and Supplemental video). These effects did not occur with the inactive DNT^{mut}-TAT (Fig. 2B). Moreover, we studied the activation of Rho GTPases in intact cells by DNT-TAT. For this purpose, BMMC were treated with DNT-TAT, and were analyzed by a pull-down assay with beads, carrying the Rac-binding domain of the Rac effector PAK. Fig. 1B shows that DNT-TAT activated Rac in a time-dependent manner. By contrast, the inactive mutant DNT^{mut}-TAT was not able to activate Rac in BMMC (Fig. 1B) or RBL cells (Fig. S1).

Next, we tested whether RhoA was also activated by DNT-TAT. However, we neither observed the typical RhoA shift nor an activation of the GTPase in the pull-down assay performed with the RhoA-binding domain of rhotekin. This was surprising, because recombinant RhoA was activated by the toxin *in vitro*. Therefore, we studied the Rho activation in HeLa cells. Also in these cells, DNT-TAT did not activate RhoA (Fig. S2A). To further clarify the specificity of our toxin fusion protein, we analyzed the activation of RhoA in the cytosol and compared it with the activation of recombinant RhoA. These studies showed that DNT-TAT was not able to activate native RhoA in the cell lysate of RBL cells. However, when recombinant Rho protein was added to the cytosolic fraction, activation by DNT-TAT was observable (Fig. S2B). Moreover, native RhoA in the lysate, which was not activated by DNT-TAT, was activated by the addition of GTPγS (Fig. S2C). This indicated that the fusion protein DNT-TAT is not able to activate native RhoA but recombinant RhoA. It remains to be clarified whether the isoprenylation of native RhoA is responsible for this substrate specificity. Thus, the findings indicate that DNT-TAT activates Rac but not RhoA in RBL cells and BMMC.

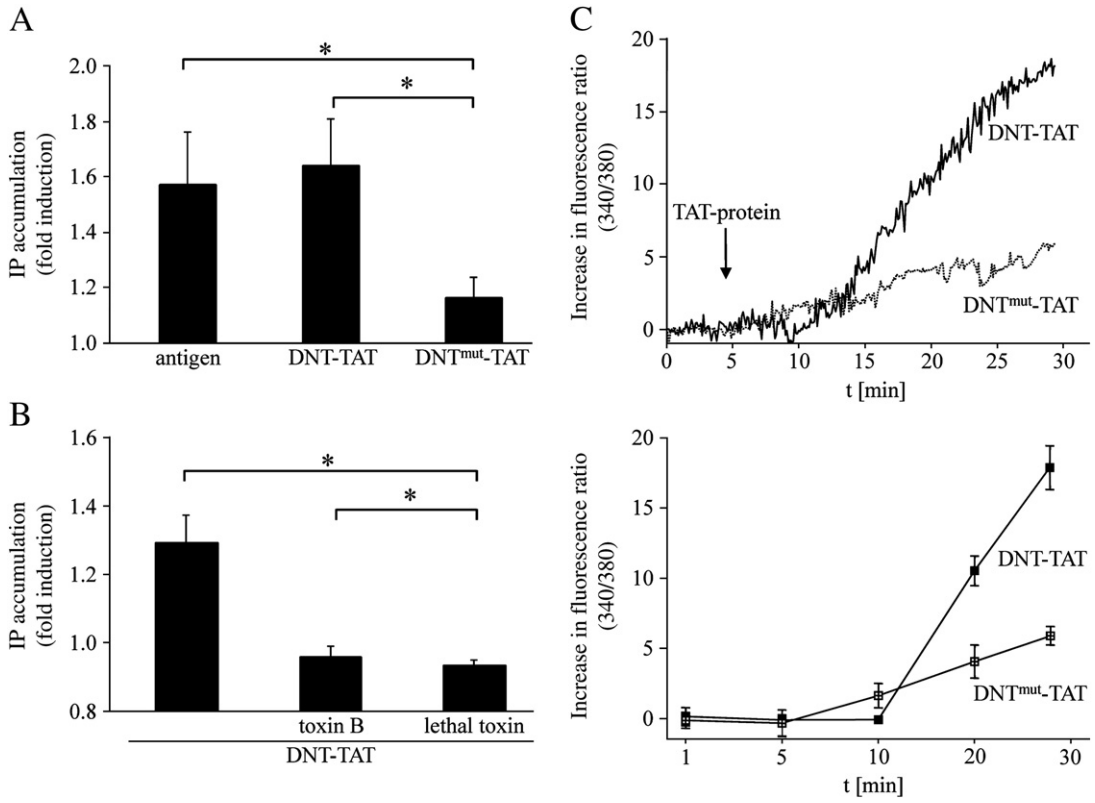

Fig. 3. Effects of DNT-TAT on the formation of inositol phosphates and calcium mobilization. A. BMMC were incubated with [2-^{3}H]inositol (4 μCi/ml) overnight. Where needed, cells were labelled with 1% anti-TNP-ovalbumin IgE overnight. Thereafter, cells were treated with 200 nM of DNT-TAT or the inactive mutant for 3 h. Additionally, cells were stimulated with antigen (1 ng/ml, 5 min). Accumulation of inositol phosphates was analyzed by anion exchange chromatography as described in Section 2. Data are given as fold induction over buffer control (data are given as means ± SD, $n = 3$). Statistical significance was assessed using a paired Student's t-test, with $^*p < 0.05$. B. BMMC were incubated with [2-^{3}H]inositol (4 μCi/ml), toxin B (30 ng/ml) and lethal toxin (200 ng/ml) overnight and, thereafter, treated with 200 nM of DNT-TAT for 3 h. Formation of inositol phosphates was measured by anion exchange chromatography. Data are calculated as fold induction to untreated cells (data are given as mean ± SD, $n = 3$). Statistical significance was assessed using a paired Student's t-test, with $^*p < 0.05$. C. RBL cells were seeded on glass-bottom culture dishes and, thereafter, loaded with Fura-2AM (2.5 μM). Cells were stimulated with 200 nM DNT-TAT or the inactive mutant DNT^{mut}-TAT, respectively. Calcium imaging was performed as described in Section 2. The results are presented as an increase in changes in fluorescence ratio 340/380 nm over time. Upper panel: shown is a typical experiment from three independent experiments with similar results. Data are given as means of 7 (DNT-TAT) and 6 cells (DNT^{mut}-TAT). The lower panel shows the means and standard deviations of indicated time points from this experiment.

3.2. Involvement of Rac in calcium mobilization

Because it is known that Rac activates PLCγ in mast cells [28], we studied the effects of DNT-TAT on inositol phosphate formation. As expected, the toxin increased the inositol phosphate accumulation by ~50%, whereas the inactive mutant did not show any effect (Fig. 3A). A similar increase in inositol phosphate accumulation was induced by treatment of IgE-loaded mast cells with TNP-ovalbumin. To test whether the increase in inositol phosphate accumulation was induced by Rac activation, we treated cells with *C. difficile* toxin B and *C. sordellii* lethal toxin, which are known to inactivate Rac [29]. Accordingly, toxin B and lethal toxin were able to block the increase in inositol phosphate accumulation induced by antigen and also by DNT-TAT, indicating a Rac-dependent effect (Fig. 3B). Activation of PLCγ results additionally in the mobilization of intracellular calcium. Thus, we tested the effects of DNT-TAT on calcium mobilization by means of calcium imaging. Similarly as observed for antigen, also DNT-TAT, but not the mutant DNT^{mut}-TAT construct, caused calcium mobilization in RBL cells (Fig. 3C). This effect was inhibited by lethal toxin, indicating the specificity of the reaction (Fig. S3A). Furthermore, EGTA, added to the cell medium, inhibited the calcium mobilization (Fig. S3B). This suggested that the intracellular calcium mobilization depended on the influx of extracellular calcium.

Moreover, we observed that the ionophore A23187 induced the activation of Rac, which was detected by the PAK pull-down assay (Fig. 4A). Because the strong calcium mobilization by A23187 might have several additional effects on mast cell activation, we treated cells with a cell permeable $InsP_3$ analog to induce selective intracellular calcium mobilization. As shown in Fig. 4B, the $InsP_3$ analog ($Bt_3Ins(1,3,4)P_3$ AM) induced an increase in intracellular calcium. This effect was inhibited by lethal toxin, again indicating the involvement of Rho family proteins.

3.3. Effects of DNT-TAT on mast cell secretion

Next, we studied whether DNT-TAT was also able to induce the degranulation of mast cells. As shown in Fig. 5A, the toxin increased the hexosaminidase release 2–3 folds as compared to controls. However, the effect on hexosaminidase release was lower than that of antigen. Lethal toxin almost completely blocked the release of hexosaminidase induced by antigen and by DNT-TAT (Fig. 5B), indicating the crucial role of Rac proteins in degranulation. Notably, the basal hexosaminidase release in RBL cells seems to be higher than in BMMC. Thus, inhibition of antigen or DNT-TAT-induced degranulation by lethal toxin in RBL cells is not that pronounced as compared to BMMC. Furthermore, activation of mast cells by A23187 was inhibited by toxin B and by lethal toxin, indicating the pivotal role of the GTPase in the activation of mast cells by A23187 (Fig. 5C).

3.4. Influence of DNT-TAT and calcium on ERK phosphorylation

Activation of mast cells by antigen causes the stimulation of the Map kinase ERK (extracellular signal-regulated kinase), a reaction which might be important for the induction of cytokine expression [30].

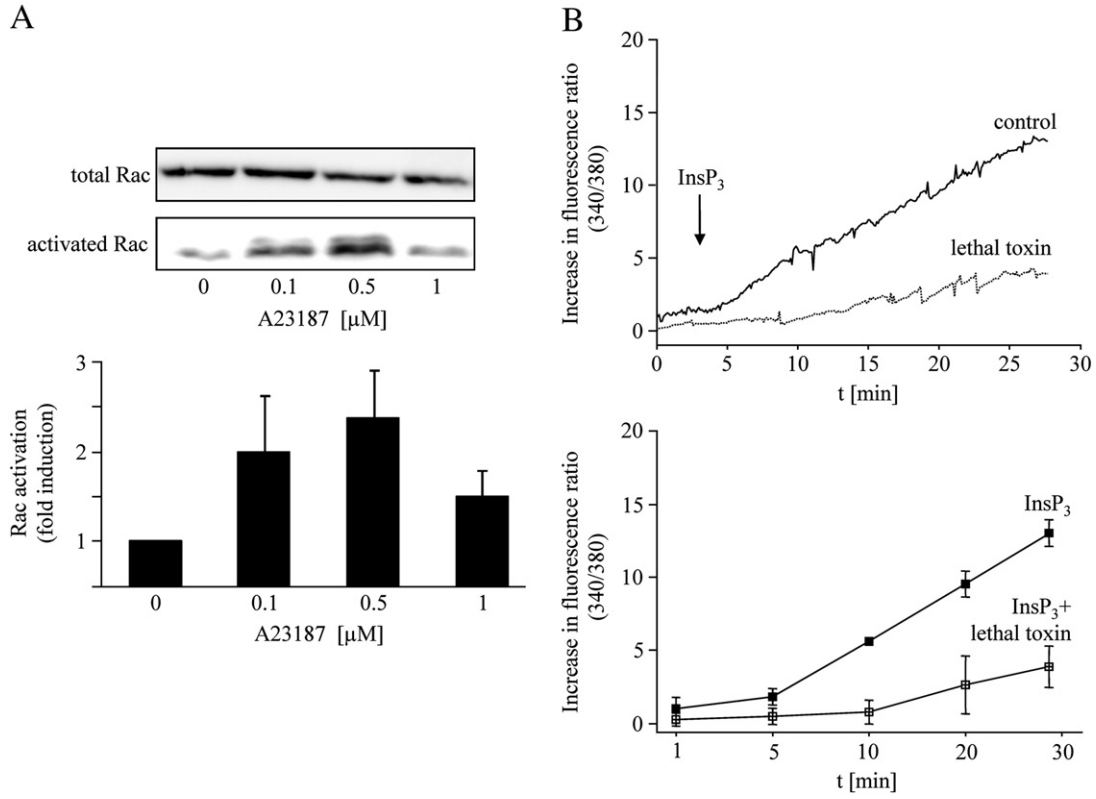

Fig. 4. Influence of A23187 and Rho GTPase inactivating toxins on calcium mobilization. A. BMMC were stimulated with increasing concentrations of A23187 for 30 min. An effector pull-down assay and a Western blot were performed to monitor Rac activation. A fraction of total lysates was used to check equal loading. Rac was detected by a specific antibody. The lower panel shows the quantification of Rac activation by measuring band intensity normalized to control, determined of three independent experiments (mean ± SD, $n = 3$). B. RBL cells were seeded on glass-bottom culture dishes and grown over night. Thereafter, cells were preincubated with lethal toxin (200 ng/ml, 2 h) and loaded with Fura-2AM. Calcium mobilization was initiated by the addition of cell permeable $InsP_3$ (50 μM, $Bt_3Ins(1,3,4)P_3$ AM) and calcium imaging was performed as described. Results are presented as an increase in changes in fluorescence ratio 340/380 nm over time. Upper panel: shown is a typical experiment from three independent experiments with similar results. Data are given as means of 6 ($InsP_3$) and 8 cells ($InsP_3$ + lethal toxin). The lower panel shows the means and standard deviations of indicated time points from this experiment.

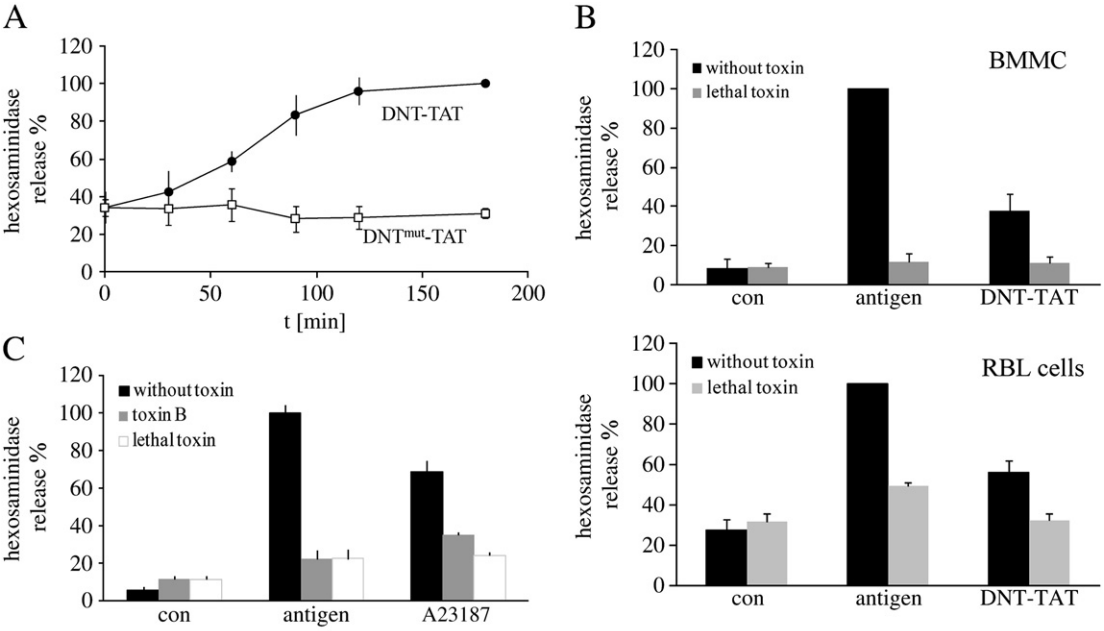

Fig. 5. Influence of DNT-TAT on mast cell secretion. A. BMMC were stimulated with 300 nM DNT-TAT or the inactive mutant for the indicated time and degranulation was measured in the supernatant. Hexosaminidase release is shown in relation to untreated cells and calculated to the maximum of DNT-TAT-induced secretion (mean ± SD, $n = 6$). B. RBL cells and BMMC were pretreated with lethal toxin (200 ng/ml) for 30 min or overnight, respectively. Where needed, cells were labelled with IgE overnight. Cells were stimulated with 300 nM DNT-TAT (1–2 h) or 1 ng/ml antigen (15 min) and hexosaminidase release was measured in the supernatant. Hexosaminidase release is shown in relation to untreated cells and calculated to the maximum of antigen-induced secretion (mean ± SD, $n = 3$). C. BMMC were pretreated with toxin B (30 ng/ml) or lethal toxin (200 ng/ml) for 16 h and, where needed, loaded with IgE. Cells were stimulated with antigen (1 ng/ml) or A23187 (0.5 μM), respectively for 30 min. Thereafter, degranulation was measured in the supernatant. Hexosaminidase release is shown in relation to untreated cells and calculated to the maximum of antigen-induced secretion (mean ± SD, $n = 3$).

Therefore, we studied whether DNT-TAT has any effects on ERK activation. As shown in Fig. 6A, the fusion toxin, but not the inactive mutant, increased the ERK1/2 phosphorylation in BMMC. This effect was less pronounced than the activation of ERK induced by antigen. Both, toxin B and lethal toxin inhibited the activation of ERK1/2 by DNT-TAT (Fig. 6B). Because the signal pathway of DNT-TAT-induced ERK activation is not well defined, we wanted to know, whether the toxin-induced calcium mobilization is sufficient for ERK activation. Therefore, we studied the effects of the calcium ionophore A23187 on ERK activation. As shown in Fig. 6C, A23187 caused a strong activation of ERK, which was inhibited by toxin B and lethal toxin. Thus, also activation of MAP kinases by A23187 was sensitive towards Rho GTPase-inactivating toxins. However, inhibition of ERK phosphorylation induced by A23187 was much stronger by lethal toxin than by toxin B (Fig. 6C).

4. Discussion

Rac is crucially involved in the activation of mast cells caused by cross-linking of FcεRI receptors by antigen [31,32]. However, cross-linking of FcεRI receptors induces a large array of signal responses, which rather propagate in signaling networks than in a single signal cascade. To learn more about the role of Rac in mast cell activation, we attempted to use selective toxins as tools to activate the GTPase independently of the up-stream FcεRI receptor. Because CNF and DNT, which both are able to activate Rho GTPases by deamidation and/or transglutamination, were not taken up by mast cells, we constructed TAT fusion proteins to get access to the intracellular compartment of target cells. To this end, a TAT fusion protein was constructed, which consisted of the catalytic domain of DNT and the TAT peptide, which is applied to allow translocation of proteins into target cells. The DNT-TAT construct activated recombinant Rac *in vitro* by deamidation and/or transglutamination. The latter reaction was verified by the attachment of dansylcadaverine onto Rac. A mutant DNT-TAT protein with a change of the catalytic cysteine residue (Cys1296Ser) in the catalytic domain of DNT was used as a control.

Treatment of RBL cells with the fusion toxin resulted in typical Rac effects [33], e.g. cell spreading, very strong membrane ruffling and lamellipodia formation. In addition we observed the formation of long cell extensions. It appeared that after toxin treatment the retraction and dynamics of the long extensions were reduced as compared to control cells. According to the Rac-like effects, we detected the activation of Rac protein in the cell lysate of RBL cells and BMMC by PAK pull-down assay. Surprisingly, we were not able to observe the activation of endogenous RhoA although recombinant RhoA was a substrate of DNT-TAT. Thus, we suggest that the fusion toxin is more specific in intact cells than *in vitro*. The predominant activation of Rac, which is also known to negatively regulate RhoA in many cell types, might be the reason why retraction of cell extensions was reduced after DNT-TAT treatment.

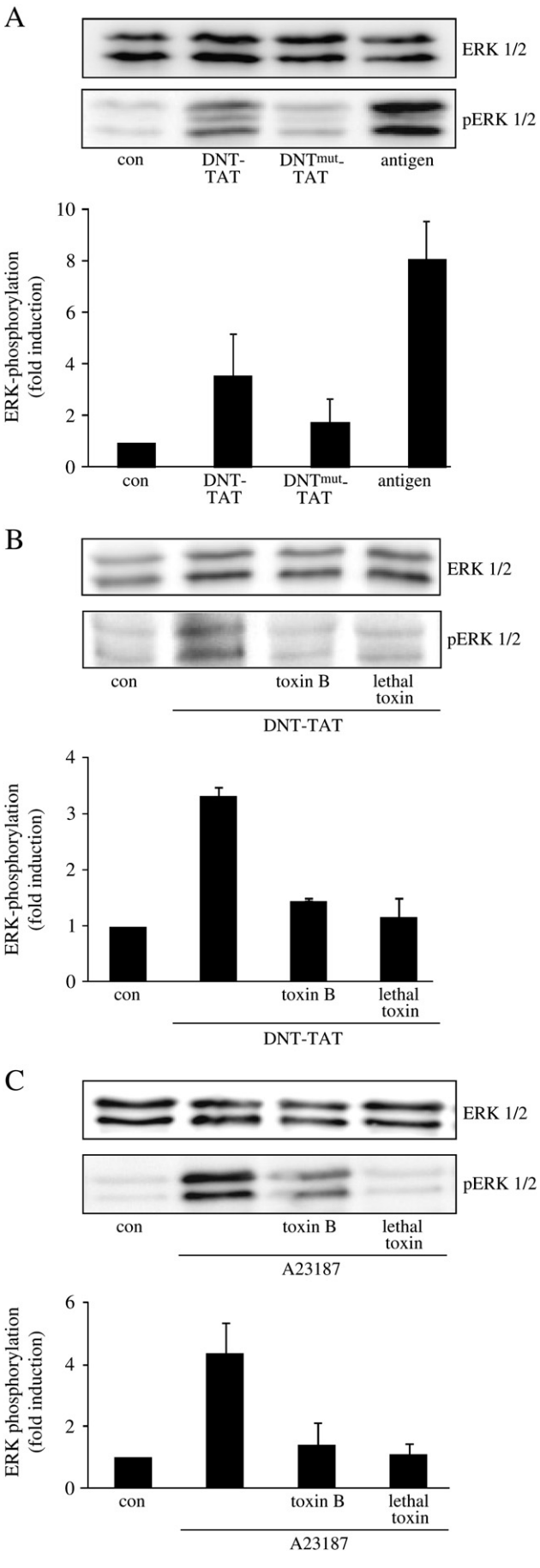

Fig. 6. Effects of DNT-TAT on ERK phosphorylation. A. Where needed, cells were loaded with IgE overnight. Thereafter, BMMC were stimulated with antigen (1 ng/ml, 10 min), incubated with 200 nM DNT-TAT or the inactive mutant for 30 min. Cells were lysed with RIPA-buffer and SDS-PAGE and Western blots were performed. ERK1/2 and phosphorylated ERK 1/2 were detected by specific antibodies. The lower panel shows the quantification of ERK 1/2-phosphorylation by measuring band intensity normalized to control (Multi Gauge V3.0 software), determined from three independent experiments (mean ± SD, $n = 3$). B. BMMC were pretreated with toxin B (30 ng/ml) or lethal toxin (200 ng/ml) overnight and, thereafter, the cells were incubated with 200 nM DNT-TAT for 20 min. After incubation, cells were treated as described in (A). The lower panel shows the quantification of ERK 1/2-phosphorylation by measuring band intensity normalized to control, determined from three independent experiments (data are given as mean ± SD, $n = 3$). C. BMMC were pretreated with toxin B (30 ng/ml, 16 h) and lethal toxin (200 ng/ml, 16 h) respectively. Cells were stimulated with calcium ionophore (A23187, 0.5 μM, 10 min). After incubation, cells were treated as described in (A). The lower panel shows the quantification of ERK 1/2 phosphorylation by measuring band intensity normalized to control, determined from three independent experiments (data are given as mean ± SD, $n = 3$).

In line with an activation of Rac and subsequent stimulation of PLCγ, we observed an increased inositol phosphate accumulation and mobilization of calcium in RBL cells and BMMC induced by DNT-TAT, which was inhibited by toxin B or lethal toxin, respectively, indicating the specificity of the DNT-TAT effects. Calcium mobilization induced by DNT-TAT depended on the presence of extracellular calcium.

We compared the effect of DNT-TAT on calcium mobilization with the activity of the calcium ionophore A23187. The ionophore caused a strong increase in intracellular calcium. Interestingly, also this effect was inhibited by Rho GTPase-inhibiting toxins like toxin B and lethal toxin, indicating the involvement of Rac. Moreover, the activation of Rac by A23187 was corroborated by the Pak pull-down assay. We also applied an $InsP_3$ analog to mobilize calcium and again the Rho-inactivating toxins inhibited its effect, verifying a role of Rac in intracellular calcium mobilization following intracellular calcium release. Another exciting question is how Rac is activated by A23187 or $InsP_3$. Collard et al. showed that an increase in cellular calcium causes Rac activation and translocation [34]. However, the precise mechanisms and the GEF proteins involved in calcium-induced activation of Rac in mast cells are not known.

DNT-TAT also caused hexosaminidase release from RBL cells and from BMMC. Again the effects by DNT-TAT were not observed with the inactive mutant fusion protein and could be blocked by Rac-inactivating toxins.

Activation of the FcεRI by antigen causes the activation of MAP kinases and phosphorylation of ERK [35]. This signaling pathway results in transcriptional regulation and may be important for the production of cytokines induced by antigen receptor activation. In addition, DNT-TAT activated ERK, indicating a signal pathway from Rac to ERK. This was corroborated by the findings that activation of ERK by DNT-TAT was inhibited by lethal toxin and toxin B. However the activation by DNT-TAT was less pronounced than that via the stimulation of the FcεRI receptor by antigen binding. This indicates that the signal network induced by cross-linking of the antigen receptor is more efficient in activating Map kinase pathways to ERK.

Mobilization of intracellular calcium may be sufficient for ERK activation. Accordingly, A23187 caused ERK phosphorylation in mast cells. Again, this effect was inhibited by toxin B and by lethal toxin. Because lethal toxin acts on Rac and in addition on Ras, whereas toxin B acts selectively on Rho GTPases, it is feasible that A23187 but not DNT-TAT causes the activation of Ras. Taken together the data indicate that Rac is not only involved in the regulation of PLCγ but also in effects downstream of $InsP_3$ or A23187-induced calcium mobilization. Recent reports suggest that production of reactive oxygen species (ROS) play a pivotal role in the activation of mast cells by inhibiting phosphatases involved in mast cell signaling [36]. Moreover ROS appear to be involved in MAP kinase activation and it has been suggested that ROS production is crucially regulated by calcium mobilization. It is well known that Rac is involved in ROS production by NADPH oxidase in several cell types [37–39]. Thus, calcium mobilization induced by stimulation of PLCγ, by the cell permeable $InsP_3$ analog or by A23187 may induce a positive feedback of mast cell signaling via ROS activation, which on the other hand depends on Rac. Therefore, stimulation of Rac by DNT-TAT or inhibition of the GTPase by inhibiting toxins like toxin B and lethal toxin would have major effects on mast cell activation. It remains to be studied whether ROS production has a pivotal role in the action of DNT-TAT on mast cells.

5. Conclusion

A fusion toxin consisting of the catalytic domain of DNT and a peptide from the TAT protein facilitates the entry of the Rho GTPase-activating toxin into target cells, which are otherwise insensitive such as RBL cells and BMMC. The toxin allows to study the role of Rac proteins in signalling independently of receptor activation (e.g. FcεRI). By means of the activating fusion toxin and with specific Rho GTPase-inactivating toxins, it is shown that Rac protein plays a central role in mast cell activation not only in receptor-mediated regulation of PLCγ but also in calcium mobilization downstream of PLCγ and in activation of ERK kinase.

Acknowledgement

The studies were financially supported by the Landesstiftung Baden-Württemberg, programme “Allergologie”.

Appendix A. Supplementary data

Supplementary data associated with this article can be found, in the online version, at doi:10.1016/j.cellsig.2010.03.007.

References

[1] D.D. Metcalfe, R.D. Peavy, A.M. Gilfillan, J. Allergy Clin. Immunol. 124 (2009) 639.
[2] S. Kraft, J.P. Kinet, Nat. Rev. Immunol. 7 (2007) 365.
[3] H. Turner, J.-P. Kinet, Nature 402 (1999) B24.
[4] V. Parravicini, M. Gadina, M. Kovarova, S. Odom, C. Gonzalez-Espinosa, Y. Furumoto, S. Saitoh, L.E. Samelson, J.J. O'Shea, J. Rivera, Nat. Immunol. 3 (2002) 741.
[5] X.R. Bustelo, Mol. Cell. Biol. 20 (2000) 1461.
[6] E. Hong-Geller, R.A. Cerione, J. Cell Biol. 148 (2000) 481.
[7] E. Hong-Geller, D. Holowka, R.P. Siraganian, B. Baird, R. Cerione, Proc. Natl Acad. Sci. U. S. A. 98 (2001) 1154.
[8] A.B. Jaffe, A. Hall, Annu. Rev. Cell Dev. Biol. 21 (2005) 247.
[9] A.J. Ridley, Trends Cell Biol. 11 (2001) 471.
[10] S. Etienne-Manneville, A. Hall, Nature 420 (2002) 629.
[11] K. Wennerberg, C.J. Der, J. Cell Sci. 117 (2004) 1301.
[12] K. Aktories, J.T. Barbieri, Nat. Rev. Microbiol. 3 (2005) 397.
[13] C. Hoffmann, G. Schmidt, Rev. Physiol. Biochem. Pharmacol. 152 (2004) 49.
[14] T. Jank, K. Aktories, Trends Microbiol. 16 (2008) 222.
[15] I. Just, J. Selzer, M. Wilm, C. Von Eichel-Streiber, M. Mann, K. Aktories, Nature 375 (1995) 500.
[16] F. Hofmann, G. Rex, K. Aktories, I. Just, Biochem. Biophys. Res. Commun. 227 (1996) 77.
[17] G. Schmidt, P. Sehr, M. Wilm, J. Selzer, M. Mann, K. Aktories, Nature 387 (1997) 725.
[18] G. Flatau, E. Lemichez, M. Gauthier, P. Chardin, S. Paris, C. Fiorentini, P. Boquet, Nature 387 (1997) 729.
[19] M. Masuda, L. Betancourt, T. Matsuzawa, T. Kashimoto, T. Takao, Y. Shimonishi, Y. Horiguchi, EMBO J. 19 (2000) 521.
[20] I. Just, J. Selzer, F. Hofmann, K. Aktories, in: K. Aktories (Ed.), Bacterial toxins — tools in cell biology and pharmacology, Chapman & Hall, Weinheim, 1997, p. 159.
[21] H.N. Eisen, S. Belman, M.E. Carsten, J. Am. Chem. Soc. 75 (1953) 4583.
[22] I. Just, G. Fritz, K. Aktories, M. Giry, M.R. Popoff, P. Boquet, S. Hegenbarth, C. Von Eichel-Streiber, J. Biol. Chem. 269 (1994) 10706.
[23] H. Karasuyama, F. Melchers, Eur. J. Immunol. 18 (1988) 97.
[24] N. Djouder, U. Prepens, K. Aktories, A. Cavalié, J. Biol. Chem. 275 (2000) 18732.
[25] C. Hoffmann, K. Aktories, G. Schmidt, J. Biol. Chem. 282 (2007) 10826.
[26] C. Busch, J. Orth, N. Djouder, K. Aktories, Infect. Immun. 69 (2001) 3628.
[27] G. Schmidt, U.-M. Goehring, J. Schirmer, S. Uttenweiler-Joseph, M. Wilm, M. Lohmann, A. Giese, G. Schmalzing, K. Aktories, Infect. Immun. 69 (2001) 7663.
[28] N. Djouder, E. Aneiros, A. Cavalié, K. Aktories, J. Pharmacol. Exp. Ther. 304 (2003) 1243.
[29] I. Just, J. Selzer, F. Hofmann, G.A. Green, K. Aktories, J. Biol. Chem. 271 (1996) 10149.
[30] K. Chayama, P.J. Papst, T.P. Garrington, J.C. Pratt, T. Ishizuka, S. Webb, S. Ganiatsas, L.I. Zon, W. Sun, G.L. Johnson, E.W. Gelfand, Proc. Natl Acad. Sci. U. S. A. 98 (2001) 4599.
[31] U. Prepens, I. Just, C. Von Eichel-Streiber, K. Aktories, J. Biol. Chem. 271 (1996) 7324.
[32] H. Turner, M. Gomez, E. Mckenzie, A. Kirchem, A. Lennard, D. Cantrell, J. Exp. Med. 188 (1998) 527.
[33] A.J. Ridley, H.F. Paterson, C.L. Johnston, D. Diekmann, A. Hall, Cell 70 (1992) 401.
[34] L.S. Price, M. Langeslag, J.P. ten Klooster, P.L. Hordijk, K. Jalink, J.G. Collard, J. Biol. Chem. 278 (2003) 39413.
[35] L.M. Sly, J. Kalesnikoff, V. Lam, D. Wong, C. Song, S. Omeis, K. Chan, C.W. Lee, R.P. Siraganian, J. Rivera, G. Krystal, J. Immunol. 181 (2008) 3850.
[36] Y. Suzuki, T. Yoshimaru, T. Matsui, T. Inoue, O. Niide, S. Nunomura, C. Ra, J. Immunol. 171 (2003) 6119.
[37] P.L. Hordijk, Circ. Res. 98 (2006) 453.
[38] A. Abo, E. Pick, A. Hall, N. Totty, C.G. Teahan, A.W. Segal, Nature 353 (1991) 668.
[39] G.M. Bokoch, B.A. Diebold, Blood 100 (2002) 2692.